Peer-reviewed version available at *Nanomaterials* **2019**, *9*, 1218; doi:10.3390/nano9091218

Article

Fabrication of crystalline microresonators of high quality factors with a controllable wedge angle on lithium niobate on insulator

Jianhao Zhang [1,2,†], Zhiwei Fang [3,4,†], Jintian Lin [1], Junxia Zhou [3,4], Min Wang [3,4], Rongbo Wu [1,2], Renhong Gao [1,2] and Ya Cheng [1,3,4,5,*]

[1] State Key Laboratory of High Field Laser Physics, Shanghai Institute of Optics and Fine Mechanics, Chinese Academy of Sciences, Shanghai 201800, China; jhzhang@siom.ac.cn (J. Z.); jintianlin@siom.ac.cn (J.L.); rbwu@siom.ac.cn (R.W.) ; rhgao@siom.ac.cn (R.G)

[2] Center of Materials Science and Optoelectronics Engineering, University of Chinese Academy of Sciences, Beijing 100049, China

[3] State Key Laboratory of Precision Spectroscopy, East China Normal University, Shanghai 200062, China; zwfang@phy.ecnu.edu.cn (Z.F.); mwang@phy.ecnu.edu.cn (M.W.); 52180920026@stu.ecnu.edu.cn (J.Z.)

[4] XXL—The Extreme Optoelectromechanics Laboratory, School of Physics and Materials Science, East China Normal University, Shanghai 200241, China

[5] Collaborative Innovation Center of Extreme Optics, Shanxi University, Taiyuan 030006, Shanxi, China

* Correspondence: ya.cheng@siom.ac.cn

† These author contributed equally to this work

Abstract: We report fabrication of crystalline microresonators of high quality (Q) factors with a controllable wedge angle on lithium niobate on insulator (LNOI). Our technique relies on femtosecond laser assisted chemo-mechanical polish which allows us to achieve ultrahigh surface smoothness as critically demanded by high Q microresonator applications. We show that by refining the polish parameters, Q factors as high as 4.7×10^7 can be obtained and the wedge angle of the LNOI can be continuously tuned from 9° to 51°.

Keywords: lithium niobate microdisk resonator; controllable wedge angle; high quality factors; chemo-mechanical polish

1. Introduction

Whispering gallery microresonators (WGM) are miniaturized optical cavities in which light waves can travel along the circular periphery with extremely low propagation losses by means of total internal reflection at the glass-air interface. So far, WGMs have been realized in various kinds of transparent materials such as liquids, polymers, glass, semiconductors and dielectric crystals [1-3]. The physical and/or optical functionalities demonstrated with WGMs include lasing, filtering, nonlinear wavelength conversion, optomechanics, cavity electrodynamics, to name only a few [4-9]. Currently, it is of high interest to realize on-chip integration of the WGMs with other photonic micro- and nanostructures. The material platforms suitable for photonic integration application include traditional semiconductors for

Peer-reviewed version available at Nanomaterials 2019, 9, 1218; doi:10.3390/nano9091218

their fabrication compatibility with CMOS approach and the emerging lithium niobate on insulator (LNOI) thanks to the rapid development of innovative solutions to produce high quality LNOI photonic structures [10-15].

Very recently, we have demonstrated fabrication of high Q LNOI microdisk resonators using chemo-mechanical polish lithography [16-18]. The Q factor was measured to be 1.46×10^7 at a wavelength around 773 nm. As a typical feature of chemo-mechanical polish, the fabricated microdisk shows an extended wedge at the rim of a wedge angle of ~9.5°. The high Q microresonators have been used to demonstrate electric tunable optomechanics [19]. Nevertheless, for most WGM applications, it is always desirable to improve the Q factor and to have the capability of controlling the dispersion property with a tunable wedge angle. This provides strong incentive for us to carry out systematic investigations for the optimizations of the Q factor and wedge angle by refining the fabrication parameters, which will be shown in detail below.

2. Experimental details

In our investigation, the LNOI microdisks of variable diameter and wedge angle were produced on a commercially available X-cut LNOI wafer (NANOLN, Jinan Jingzheng Electronics Co., Ltd.). The LN thin film with a thickness of 900 nm is bonded to a 2 μm-thick SiO_2 layer supported by a 500-μm-thick LN substrate.

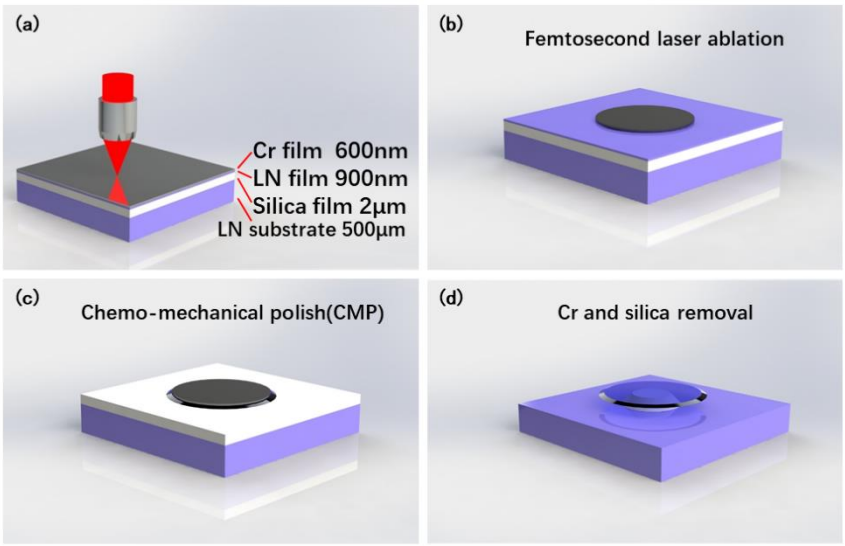

Figure 1. (**a**)-(**d**) Flowchart of fabricating an on-chip lithium niobate microdisk resonator.

As shown in Figure 1, the fabrication process includes four steps as briefly described as follows: (a) deposition of a thin layer of chromium (Cr) with a thickness of 600 nm on the surface of the LNOI by magnetron sputtering; (b) the patterning of Cr film using femtosecond laser ablation. The pulse energy of the femtosecond laser was carefully adjusted so as to enable a complete removal of the Cr film without damaging the underneath LNOI, because the damage threshold of LNOI is significantly higher than Cr under the irradiation of femtosecond laser pulses. The details in the femtosecond laser ablation are provided herein. We used a femtosecond laser with a center wavelength of 1030 nm and a pulse width of 170 fs (PHAROS, LIGHT CONVERSION) for patterning the Cr film at the average power of 0.1 mW. A 100×

Peer-reviewed version available at Nanomaterials 2019, 9, 1218; doi:10.3390/nano9091218

objective lens (M Plan Apo NIR, Mitutoyo Corporation, NA0.7) was used to produce a tightly focused spot of ~ 1 μm diameter.

In the CM polishing process using a wafer-polishing machine (NUIPOL802, Kejing, Inc.), the wedge angle can be controlled by changing the duration of the polishing process. More details of CM polishing can be found elsewhere [16-17].

3. Results and discussion

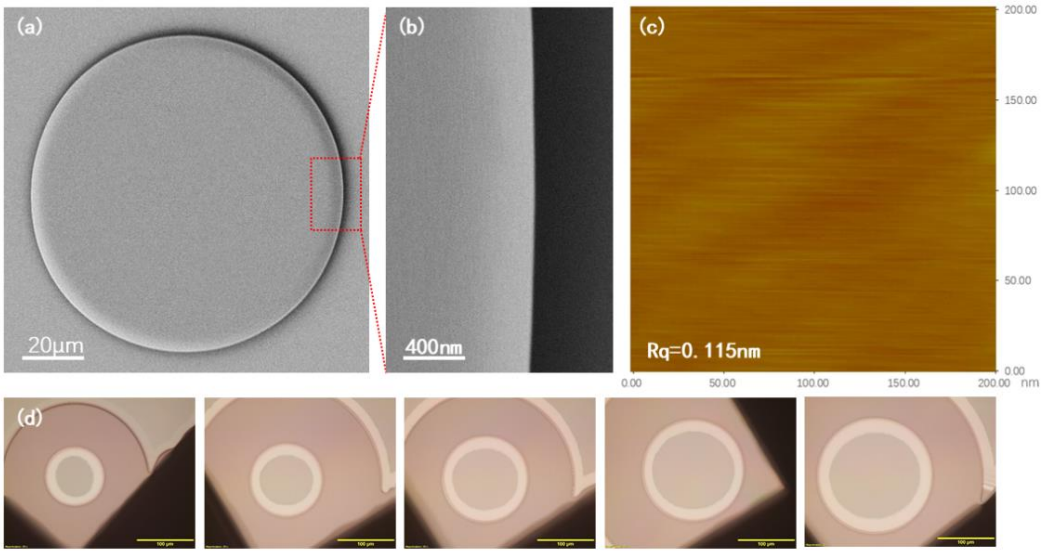

Figure 2. (**a**) Top view scanning electron microscope(SEM) image of a fabricated LN microdisk resonator. (**b**) Close up view SEM image of the area indicated by the red box in (**a**). (**c**) atomic force microscope(AFM) image of microdisk wedge. (**d**) optical microscope image of microdisk resonator with different diameters (55 μm, 85 μm, 105 μm, 135 μm, 155μm, 185 μm, 205 μm).

Figure 2a shows a LNOI microdisk fabricated using SiO_2 syrus of a particle size of ~20 nm. The close-up view of the area indicated by the red rectangular frame is shown in Figure 2b, presenting a smooth surface morphology in the optical micrograph. Figure 2c presents the atomic force microscope (AFM) image of the polished surface by which an ultralow surface roughness of Rq~0.115 nm can be determined. The surface roughness is significantly lower than that reported in our previous work (Rq~0.452 nm) owing to the fact that the syrus of particle size of ~60 nm was used previously [16]. Actually, we have systematically examined the surface roughness on the particle size and found out that a particle size of ~20 nm can give us the optimum surface roughness and a reasonable polish duration. Figure 2d exhibits all the microresonators of different diameters ranging from 55 μm to 205 μm. All the microresonators show a highly reproducible smooth surface morphology.

With a surface roughness on the order of Ra~0.115, the major source of optical loss in the microresonator is the radiative bending loss which can be reduced by increasing the diameters of the microdisks. To confirm this, we measured the Q factor of each microresonator in Figure 2d. The results are presented in Figure 3a. Indeed, it can be seen that the Q factor does undergo an increase for the microdisks of diameters 55 μm, 85 μm and 105 μm. However, after the Q factor reaches its peak, which is 4.7×10^7 obtained with the microdisk of a diameter of 105 μm, the Q factor decreases with the further increase of the diameter of the microdisk. It should be noted that to avoid the fluctuations of the measured Q factors resulting from the inconsistency

in the fabrication process, we have fabricated three samples for each diameter, and then made three measurements accordingly. The general trend in Figure 3a is therefore a reliable feature of the Q factor dependence on the microdisk diameter.

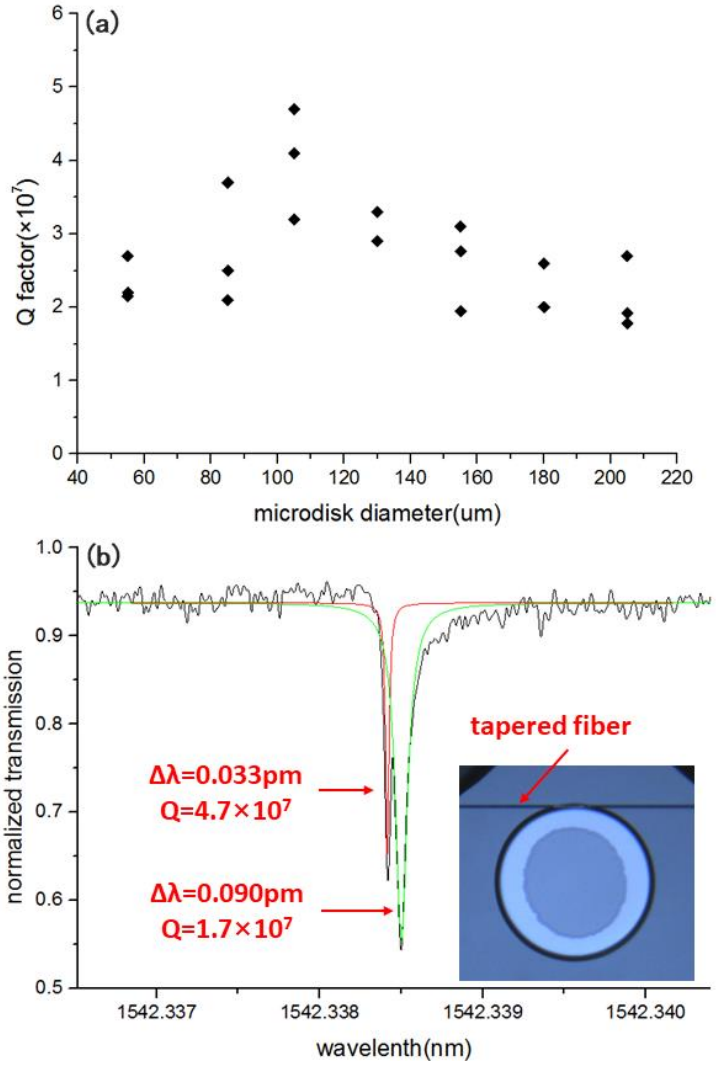

Figure 3. (**a**) The Lore ntz fitting (red curve) of a splitting mode in the microdisk of a diameter of 105 μm, reveals a Q factor of 4.7×10^7. (**b**) Measured Q factors of the mcirodisks of different diameters.

We attempt to understand the unexpected trend of the decreasing Q factor with the increasing microdisk diameter after the diameter of the microdisk reaches 105 μm. For this purpose, we carry out simulations of the light fields in the microdisks of different diameters. Note that we are not going to calculate the Q factors of the microdisks of different diameters as many key parameters (such as the exact diameter, thickness, and surface roundness of each microdisk) cannot be measured with absolute precisions. The simulation results in Figure 4 reveal that with the increase of the diameter of the microdisk, the fundamental (Figure 4a-c) and high-order (Figure 4d-f) modes tend to penetrate more deeply toward the center of the microdisk. It is highly likely that the tail of the fundamental as well as high-order modes in the microdisks of large diameters may scratch the underneath pedestal supporting the freestanding microdisk, giving rise to the decrease in the Q factors. In our work, the diameter of the fused silica pedestal is controlled to be ~20 μm less than that of the microdisk; otherwise

Preprints (www.preprints.org) | NOT PEER-REVIEWED | Posted: 25 July 2019 doi:10.20944/preprints201907.0283.v1

Peer-reviewed version available at Nanomaterials 2019, 9, 1218; doi:10.3390/nano9091218

the freestanding microdisk may collapse in the chemical wet etching for partially removing the underneath fused silica. For this reason, some fused silica may remain unremoved on the backside of the microdisk during the short period of chemical wet etching, giving rise to a slight scattering loss and in turn the slight decrease of the Q factors.

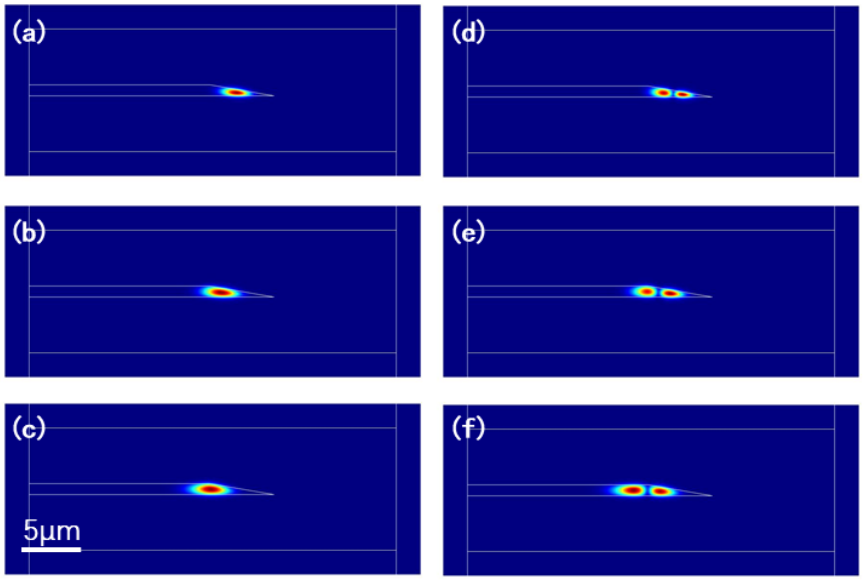

Figure 4. Fundamental modes in microdisk resonator of a diameter of (a) 50 μm, (b) 100μm, (c) 200 μm. Second-order modes in microdisk resonator of a diameter of (d) 50 μm, (e) 100μm, (f) 200 μm.

We also investigate the dependence of the wedge angle of the microdisk on the polish duration. In general, the longer the polish process, the larger the wedge angle of the microdisk. Figure 5a-f shows that the microdisks of a diameter of 85 μm obtained with polish durations of 12 mins, 16 mins, 18 mins, 24mins, 30mins, 42mins and 60mins respectively. Accordingly, the wedge angles of the microdisks in Figure 5a-f are measured to be 9°, 14°, 22°, 30°, 40° and 51°, respectively. The measured Q factors of the microdisks of different wedge angles are provided in Figure 5g. The Q factors show almost no dependence on the wedge angle, and are significantly higher than 1×10^7 at all the wedge angles.

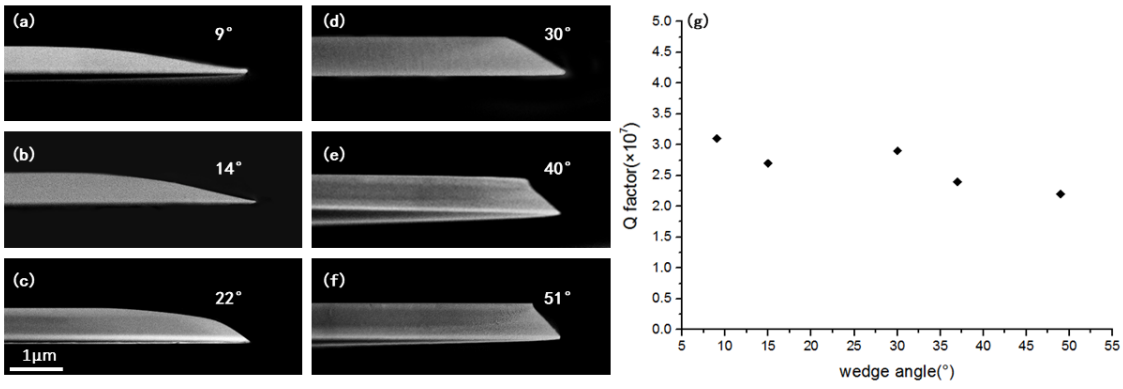

Figure 5. (a)-(f) Side view scanning electron microscope(SEM) image of fabricated LN microdisks with different wedge angles of 9°, 14°, 22°, 30°, 40° and 51°, respectively. (g) Q factors of microdisks of the different wedge angles.

At last, we notice that from the side-view image in Figure 6, the microdisks of large wedge

angles obtained with long polish durations appear to be composed of a microdisk of a vertical sidewall (see, region I in Figure 6) stacked on top of another microdisk with an extended wedge (see, region II in Figure 6). The thicknesses of region I and II are measured to be 280 nm and 420 nm, respectively. In general, this should be caused by the mechanical interaction of the LNOI microdisks with the polishing cloth, whereas understanding the underlying details requires further investigations in a systematic manner. Nevertheless, such complex geometry may provide innovative opportunities of controlling light fields in the LNOI microdisk resonators.

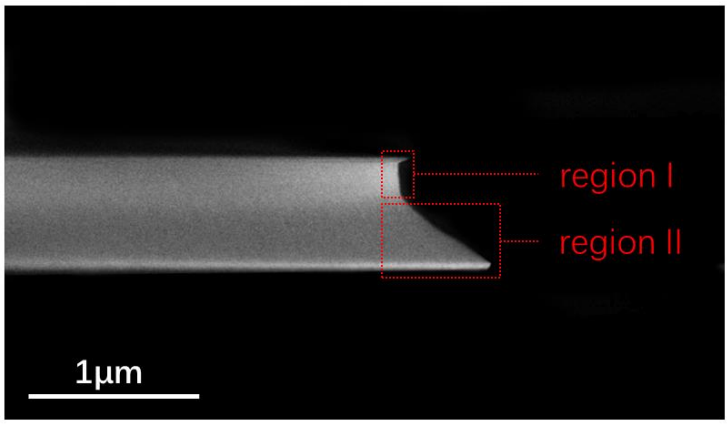

Figure 6. Side view scanning electron microscope (SEM) image of a fabricated LN microdisk resonator with a long polish duration of 90mins.

4. Conclusion

To conclude, we demonstrate optimization of the Q factor and wedge angle of LNOI microdisk resonators fabricated by femtosecond laser assisted chemo-mechanical polish. We achieve, to the best of our knowledge, a record-high Q factor of 4.7×10^7 by improving the surface smoothness and optimizing the diameter of the LNOI microdisk resonator. We show that the wedge angle of the LNOI can be continuously tuned from 9° to 51° without spoiling of the Q factor, which is critical for nonlinear optical applications as the dispersion curve in the microdisks is a function of the wedge angle. Thus, our results have important implication for applications ranging from classical and non-classical light sources to optical comb generation and optomechanics.

Author Contributions: conceptualization, Y.C.; methodology, Y.C.; software, J.Z.; validation, J.Z. and Z.F.; formal analysis, J.Z.; investigation, J.Z., J.L. and Z.F.; resources, J.Z., M.W., Z.F., R.W., J.Z.(Junxia Zhou), R.G, and J.L.; data curation, Z.F. and M.W.; writing—original draft preparation, Y.C. and J.Z.; writing—review and editing, Y.C., J.Z., M.W.,J.L. R.G. and R.W.; visualization, J.Z., J.Q., and M.W.; supervision, Y.C.; project administration, L.Q..; funding acquisition, Y.C., J.L.

Funding: This research was funded by the National Natural Science Foundation of China (Grant Nos. 11734009, 11874375, 61590934, 61635009, 61505231, 11604351, 11674340, 61575211, 61675220, 61761136006), the Strategic Priority Research Program of Chinese Academy of Sciences (Grant No. XDB16030300), the Key Research Program of Frontier Sciences, Chinese Academy of Sciences (Grant No. QYZDJ-SSW-SLH010), the Project of Shanghai Committee of Science and Technology (Grant No. 17JC1400400), the Shanghai Rising-Star Program (Grant No. 17QA1404600), National Key R&D Program of China(Grant No. 2018YFB0504400) and the Shanghai Pujiang Program (Grant No.18PJ1403300).

Conflicts of Interest: The authors declare no conflict of interest.

References:

1. Vahala, K. J.; Optical microcavities. *Nature* **2003**, 424, 839–846.
2. Jiang, X. F.; Zou, C. L.; Wang, L.; Gong, Q.; Xiao, Y.-F.; Whispering-gallery microcavities with unidirectional laser emission. *Laser & Photonics Reviews* **2016**, 10(1): 40-61.
3. Lin G.; Chembo Y. K.; Monolithic total internal reflection resonators for applications in photonics. *Optical Materials: X* **2019,** 100017.
4. Spillane S. M.; Kippenberg T.J.; Vahala K. J.; Ultralow-threshold Raman laser using a spherical dielectric microcavity. *Nature* 2002, 415, 621-623.
5. Feng, S.; Lei, T.; Chen, H.; Luo, X.; Poon, A.W.; Silicon photonics: from a microresonator perspective. *Laser & photonics reviews* **2012**, 6, 145-177.
6. Kippenberg, T. J.; Vahala, K. J.; Cavity optomechanics: back-action at the mesoscale. *Science* **2008**, 321, 1172-1176.
7. Foreman, M. R.; Swaim, J. D.; Vollmer, F.; Whispering gallery mode sensors. *Advances in optics and photonics* **2015**, 168-240.
8. Lin, G.; Coillet, A.; Chembo, Y. K.; Nonlinear photonics with high-Q whispering-gallery-mode resonators. *Advances in Optics and Photonics* **2017**, 9, 828-890.
9. Spillane, S. M.; Kippenberg, T. J.; Painter, O. J.; Vahala, K. J.; Ideality in a fiber-taper-coupled microresonator system for application to cavity quantum electrodynamics. *Physical Review Letters* **2003**, 91, 043902.
10. Lin, J.; Xu, Y.; Fang, Z.; Wang, M.; Song, J.; Wang, N.; Qiao, L.; Fang, W.; Cheng, Y. Fabrication of high-Q lithium niobate microresonators using femtosecond laser micromachining. *Scientific reports* **2015**, *5*, 8072.
11. Wang, J.; Bo, F.; Wan, S.; Li, W.; Gao, F.; Li, J.; Zhang, G.; and Xu, J.; High-Q lithium niobate microdisk resonators on a chip for efficient electro-optic modulation. *Optics express* **2015**, 23, 23072-23078.
12. Liang, H.; Luo, R.; He, Y.; Jiang, H.; Lin, Q. High-quality lithium niobate photonic crystal nanocavities. *Optica*, **2017**, 4,1251-1258.
13. Boes, A.; Corcoran, B.; Chang, L.; Bowers, J.; Mitchell, A. Status and potential of lithium niobate on insulator (LNOI) for photonic integrated circuits. *Laser Photonics Reviews* **2018**, *12*, 1700256.
14. Lin, J.; Yao, N.; Hao, Z.; Zhang, J.; Mao, W.; Wang, M.; Chu, W.; Wu, R.; Fang, Z.; Qiao, L. Broadband Quasi-Phase-Matched Harmonic Generation in an On-Chip Monocrystalline Lithium Niobate Microdisk Resonator. *Physical review letters* **2019**, *122*, 173903.
15. Zheng, Y.; Fang, Z.; Liu, S.; Cheng, Y. Chen, X.; High-Q Exterior Whispering-Gallery Modes in a Double-Layer Crystalline Microdisk Resonator. *Physical Review Letters*, **2019**, 122, 253902.
16. Wu, R.; Zhang, J.; Yao, N.; Fang, W.; Qiao, L.; Chai, Z.; Lin, J.; Cheng, Y. Lithium niobate micro-disk resonators of quality factors above 10^7. *Optics Letters* **2018**, *43*, 4116.
17. Wu, R.; Wang, M.; Xu, J.; Qi, J.; Chu, W.; Fang, Z.; Zhang, J.; Zhou, J.; Qiao, L.; Chai, Z.; et al. Long Low-Loss-Lithium Niobate on Insulator Waveguides with Sub-Nanometer Surface Roughness. *Nanomaterials* **2018**, *8*, 910.
18. Wang, M.; Wu, R.; Lin, J.; Zhang, J.; Fang, Z.; Chai, Z.; Cheng, Y. Chemo-mechanical polish lithography: A pathway to low loss large-scale photonic integration on lithium niobate on insulator. *Quantum Engineering* **2019**, *1*, e9.
19. Fang, Z.; Haque, S.; Lin, J.; Wu, R.; Zhang, J.; Wang, M.; Zhou, J.; Rafa, M.; Lu, T.; Cheng, Y. Real-time electrical tuning of an optical spring on a monolithically integrated ultrahigh Q lithium nibote microresonator. *Optics Letters* **2019**, *44*, 1214.